International Journal of Automotive Technology, Vol. 20, No. 1, pp. 109–118 (2019)
DOI 10.1007/s12239–019–0010–2

pISSN 1229–9138/ eISSN 1976–3832

MINIMUM TIME LANE CHANGING PROBLEM OF VEHICLE HANDLING INVERSE DYNAMICS CONSIDERING THE DRIVER'S INTENTION

Xinglong Zhang, Youqun Zhao*, Wenxin Zhang, Fen Lin and Haiqing Li

College of Energy and Power Engineering, Nanjing University of Aeronautics and Astronautics, Nanjing 210016, China

(Received 17 October 2017; Revised 3 May 2018; Accepted 26 July 2018)

ABSTRACT–By solving driver's optimal handling input, this paper presents a novel Lane Changing Assistance System (LCAS) which can provide guidance for driver's lane changing behavior. In addition, vehicle handling inverse dynamics method is proposed to solve driver's optimal handling input. Firstly, to recognize driver's lane changing intention and decrease the false alarm rate of LCAS, a lane changing intention recognition model is established. Secondly, the handling inverse dynamics model is established; and then the inverse dynamics problem is converted into the optimal control problem. Finally, the optimal control problem is converted into a nonlinear programming problem based on GPM; then sequential quadratic programming (SQP) is applied to get the solution. The direct collocation method (DCM) is used as the contrast verification of GPM. The simulation results show that the driver's optimal handling input can be obtained according to driver's lane changing intention in the proposed LCAS; and GPM has higher computational accuracy compared with DCM. This method may provide a reference for the research of LCAS and unmanned vehicles.

KEY WORDS : Lane changing assistance, Lane changing intention, Handling inverse dynamics, Minimum time handling input

NOMENCLATURE

c : penalty coefficient
g : kernel function parameter
ω_r : yaw rate, deg^{-1}
v : lateral velocity, m·s^{-1}
u : longitudinal velocity, m·s^{-1}
m : vehicle total mass, kg
F_{yf} : cornering force of the front wheel, N
δ : steering angle of the front wheel, deg
δ_{sw} : steering wheel angle, deg
δ_r : steering wheel angle rate, deg^{-1}
F_{yr} : cornering force of the rear wheel, N
I_z : rotational inertia around vertical axis, kg·m^2
F_{xr} : braking force, N
F_{xf} : driving / braking force of the front wheel, N
θ : course angle, deg
a : distance from mass center to front axle, m
b : distance from mass center to rear axle, m
F_f : rolling resistance, N
F_w : air resistance, N
C_D : air resistance coefficient
A : frontal area, m^2
φ : road adhesion coefficient
F_{zf} : vertical force of the front wheel, N
F_{zr} : vertical force of the rear wheel, N
g_0 : gravity acceleration, m·s^{-2}
k_1 : synthesized stiffness of front wheel, N·rad^{-1}
k_2 : synthesized stiffness of rear wheel, N·rad^{-1}
h_g : centroid height, m
i : steering gear ratio
t_0 : initial time, s
t_e : terminal time, s
a_y : lateral acceleration, m·s^{-2}

*Corresponding author. e-mail: yqzhao@nuaa.edu.cn

1. INTRODUCTION

As a typical driving behavior, lane changing can not be avoided. According to statistics, 4 % ~ 10 % traffic accidents were related to improper lane changing behavior. About 75 % of them were caused by human factors. Although the mortality caused by lane changing was relatively low, lane changing conflicts were responsible for 10 % of all crash-caused traffic delays (Chovan *et al*., 1994). In 2015, about 451000 vehicles were involved in injury crashes during lane changing and merging in the United States (NHTSA, 2017). The safety of lane changing is the key problem. Advanced driver assistance system (ADAS), which is devoted to improve safety and riding comfort, has been receiving increasingly more attention in

recent years (Guo *et al*., 2016). As an important part of ADAS, the development of Lane Changing Assistance System (LCAS) can reduce the potential risk in the process of lane changing. Therefore, it is of great practical significance and theoretical research value to carry out research on LCAS.

For decades, researchers have been studying on lane changing. In 1986, the framework of lane changing decision making was established (Gipps, 1986). On this basis, many classic lane changing models were proposed. Such as MITSIM (Yang and Koutsopoulos, 1996), MRS (Zhang *et al*., 1998), SITRAS (Hidas, 2002), CORSIM (Yang and Zhou, 2004) and minimum safety spacing model (Jula *et al*., 2000). Based on theses models, lane changing warning systems were established. HLCA system (Ruder *et al*., 2002), LCA/BSD system (Stein *et al*., 2000) and ELA system (Eidehall *et al*., 2005) are three typical lane changing warning systems. The above systems usually use the turn signals as the start signal for lane changing. However, in the United States, the turn signal usage rate was approximately 44 % (Lee *et al*., 2004). And in China, the turn signal usage rate was less than 40 % (Dang *et al*., 2013). Low opening rate will increase the false alarm rate in practical application. Thus, the reliability of LCAS will be reduced.

In recent years, the accuracy of the driver's intention recognition model has been continuously improved (Berndt and Dietmayer, 2009; Doga *et al*., 2011; Gadepally *et al*., 2014; Li *et al*., 2016; Mccall *et al*., 2007; Zong *et al*., 2009). In order to reduce the false alarm rate of ADAS, researchers have been studying on the combination of ADAS and driver's intention recognition model (Xia *et al*., 2017; Xiong *et al*., 2016). The Vision Sense system, developed by the AIDA research center of Twente University in Holland, established a two-step safety early warning algorithm to ensure the real-time warning during lane changing process. That is, recognize the lane changing intention first; then estimate the risk of lane changing (Van Dijck and Van Der Heijden, 2005). Hou *et al*. (2014) established a LCAS, which integrate the minimum risk bayesian classification and decision tree model to classify and recognize the behavior of vehicles at the next moment. The extensive studies indicate that the combination of LCAS and driver's intention recognition model can effectively decrease the false alarm rate of LCAS. However, previous studies mainly focused on lane changing warning. The driver's handling input were not considered. Because of driver's improper handling input, the traffic accidents may occurred even if the lane changing environment is safe. This is not conducive to the safety of lane changing.

In order to compensate for the shortcomings of the existing LCAS, a novel LCAS which can provide handling guidance for the driver is established by solving the driver's optimal lane changing handling input. Usually, the driver-vehicle-road closed loop system is used to solve the driver's handling input problem (Cole, 2012; Guo, 1984; Guo *et al*., 2012, 2018b, 2018c; Na and Cole, 2016). Considering the different steering parameters, Wang *et al*. (2017) proposed a gain-scheduling, robust, shared steering controller to help the driver track the reference trajectory. Simulation results show that the controller can reduce driver's steering delay time of the driver-vehicle system in emergent maneuvers,especially for the inexperienced drivers. Guo *et al*. (2018a) produced a collision-free trajectory using modified artificial potential field approach, and an adaptive neural network-based backstepping tracking control method was proposed to deal with the characteristics of coupled and parameter uncertainties for autonomous vehicles, the results show that the proposed method has excellent tracking performance. The above methods can be regarded as "positive problem" in vehicle handling dynamics. In contrast to the "positive problem", the research approach of vehicle handling inverse dynamics is to obtain the driver's handling input under the condition that the vehicle model and the motion state are known; and then analyze what kind of manipulation is the most acceptable, safest and fastest for most drivers (Wang *et al*., 2014). Bernard and Pickelmann (1986) presented a nonlinear inverse model of a vehicle which simulates combined steering and braking/driving, the results show that the inverse method is useful in solving the problem of path tracking under different braking/driving. It provides a new idea for the development and application of vehicle handling dynamics. Fujioka and Kimura (1992) used the transient vehicle dynamics model to represent the vehicle with different driving and steering configurations, and the conjugate gradient descent method was used to solve the minimum time handling problem that the starting point, the end point and the trajectory is not constraint. However this would not happen so universally in general. Hendrikx *et al*. (1996) studied the optimal handling inverse problem by applying optimal control theory and Pontryagin's minimum principle, the results show that different configurations of vehicles have different optimal control strategies, and this method can evaluate the optimal transient handling performance of the vehicles. This algorithm is rather robust with respect to inaccurate starting values, but it is the least efficient in terms of speed of convergence. Casanova *et al*. (2000) established a vehicle steering control model based on the linear optimal discrete time preview control theory, and obtained the control input and optimal completion time by using inverse dynamics method. Andreasson and Bunte (2006) used the inverse dynamics method to study the vehicle chassis control, the results show that this method is an effective method for dealing with the complex problems of chassis control. Boyer and Ali (2011) used the handling inverse dynamics method to study the multi-body dynamics of the vehicle and analyzed the maneuverability of the vehicle. Wang *et al*. (2015) used the multiple shooting methods to study the emergency collision avoidance problem, However, the linearization in this method makes the quadratic

programming problem deviate to a great extent from the original model. Liu and Jiang (2016) used pseudospectral method to study the optimal path tracking control problem. This method shows many advantages compared to the traditional methods. With the development of the application of pseudospectral methods, pseudospectral methods have gradually become the most active branch of the numerical solution method for optimal control problem (Garg *et al*., 2011).

In summary, in order to improve the safety of lane changing and handle with the parameter uncertainties of driver model. The main contributions of this paper are:

1. To deal with the characteristic of parameter uncertainties for driver modeling, a handling inverse dynamics model consisting of vehicle motion model and optimal control model is established.

2. A GPM-based solving method is presented to produced the desired optimal lane changing input; besides, the computational accuracy and efficiency of GPM is proven by DCM.

3. To avoid traffic accidents caused by driver's improper handling, a novel LCAS which can provide handling guidance for driver's lane changing behavior according to driving intention is constructed.

The paper is structured as follows. The hybrid intention recognition model based on HMM-SVM is established in Section 2. The vehicle handling inverse dynamics model of minimum time lane changing is proposed in Section 3. Section 4 converts the vehicle inverse dynamics problem into optimal control problem, and then the solution method is put forward. Section 5 discusses the contrast verification and simulation results. Conclusions are drawn in Section 6.

2. INTENTION RECOGNITION MODEL

To improve the effectiveness of LCAS, a hybrid HMM-SVM model is established. The HMM model does the preliminary recognition according to the driver's input and the vehicle state; then the maximum likelihood estimate is output. The SVM model does the secondary recognition according to the maximum likelihood estimate; and then the lane changing intention can be obtained.

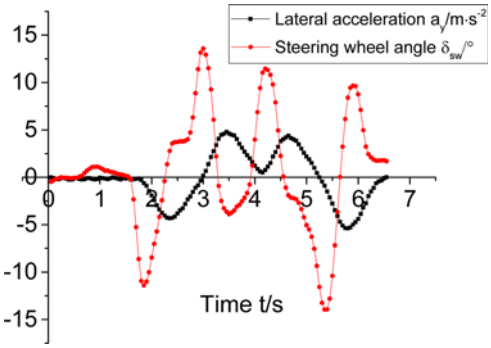

Figure 1. Part of experimental data.

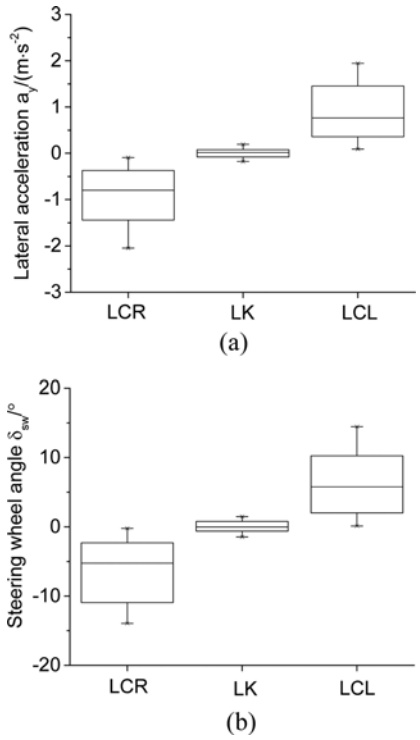

Figure 2. (a) Boxplot of lateral acceleration; (b) Boxplot of steering wheel angle.

The steering wheel angle sensor signal and the lateral acceleration signal generated by the driver's hardware in the loop test bench are used as sequence signals.

The proposed LCAS mainly focuses on the driver's intention recognition at the initial stage of lane changing, and guides the driver to complete lane changing operation according to the driving intention. Therefore, it is necessary to intercept the lane changing data for training the driver's intention recognition model. Figure 2 shows the boxplot obtained from the intercepted data.

It can be seen from Figure 2 that the differences between

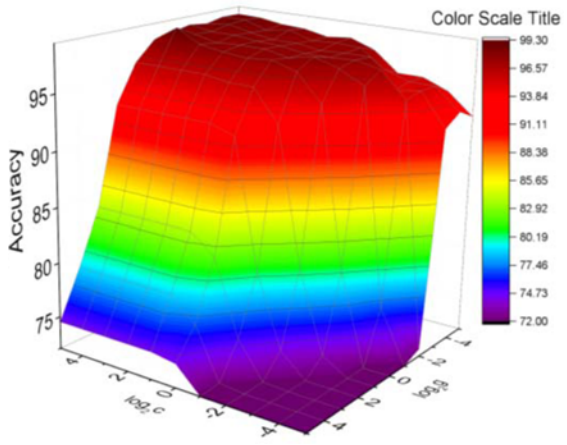

Figure 3. Cross validation results.

the data of LCR (Lane Changing Right), LK (Lane Keeping) and LCL (Lane changing Left) are remarkably, and the obvious difference is helpful to improve the recognition accuracy of the intention recognition model.

In order to obtain the best classification results, it is necessary to seek an optimal combination of c and g in the SVM model. Figure 3 illustrates that the accuracy of SVM model varies with parameters. The optimal value of c and g are 16 and 0.0313, respectively. The corresponding optimal accuracy is 99.237 %; and the recognition time is 0.017 s. The data of LCL, LCR and LK are selected to test the driver's lane changing intention recognition model, and the recognition results are as follows:

The simulation results of driver's intention recognition are shown in Figures 4 (a) ~ (c), where 0 represents lane keeping intention, 1 represents lane changing left intention, −1 represents lane changing right intention. It can be seen that if the steering wheel angle changes too much during the process of lane keeping, the driver's intention recognition model will erroneously assumed that the driver has lane changing intention, but with the subsequent operation of the driver, the intention recognition model corrects the recognition result. Thus, it can be conclude that during the process of lane changing, the driver's intention recognition model can identify the driver's lane changing intention accurately.

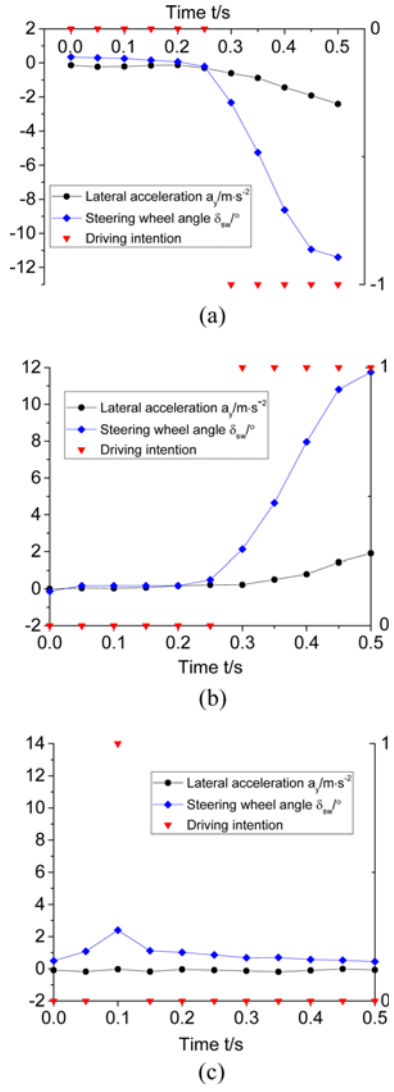

Figure 4. (a) Simulation results of LCR; (b) Simulation results of LCL; (c) Simulation results of LK.

3. HANDLING INVERSE DYNAMICS MODEL

3.1. Vehicle Motion Model

Assuming that the tire cornering properties are within the linear range, the vehicle steering motion model is simplified as a 3-degree of freedom (DOF) linear vehicle model (Liu and Jiang, 2016; Wang *et al*., 2015) with lateral motion, yawing motion and longitudinal motion, as shown in Figure 5.

The differential equations of motion can be expressed as follows:

$$\begin{cases} \dot{v} = -u\omega_{\mathrm{r}} + \dfrac{F_{\mathrm{yf}}\cos\delta + F_{\mathrm{yr}} + F_{\mathrm{xf}}\sin\delta}{m} \\ \dot{\omega}_{\mathrm{r}} = \dfrac{aF_{\mathrm{yf}}\cos\delta - bF_{\mathrm{yr}} + aF_{\mathrm{xf}}\sin\delta}{I_z} \\ \dot{u} = v\omega_{\mathrm{r}} + \dfrac{F_{\mathrm{xf}}\cos\delta - F_{\mathrm{yf}}\sin\delta + F_{\mathrm{xr}} - F_{\mathrm{f}} - F_{\mathrm{w}}}{m} \end{cases} \tag{1}$$

Considering the influence of the driving/braking force, F_{yr} and F_{yf} can be expressed as:

$$\begin{cases} F_{\mathrm{yf}} = k_1\left(\dfrac{v + a\omega_{\mathrm{r}}}{u} - \delta\right)\sqrt{1 - \left(\dfrac{F_{\mathrm{xf}}}{\varphi F_{\mathrm{zf}}}\right)^2} + \left(\dfrac{F_{\mathrm{xf}}}{k_1}\right)^2 \\ F_{\mathrm{yr}} = k_2\left(\dfrac{v - b\omega_{\mathrm{r}}}{u}\right)\sqrt{1 - \left(\dfrac{F_{\mathrm{xr}}}{\varphi F_{\mathrm{zr}}}\right)^2} + \left(\dfrac{F_{\mathrm{xr}}}{k_2}\right)^2 \end{cases} \tag{2}$$

Considering the longitudinal load transfer, F_{zr} and F_{zf} are given by:

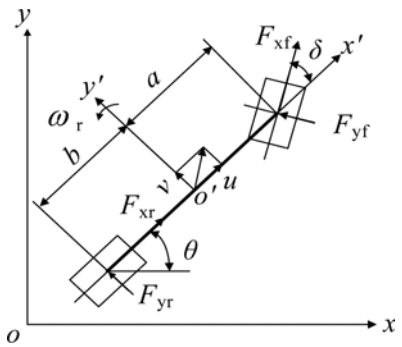

Figure 5. 3-DOF vehicle model.

$$\begin{cases} F_{zf} = \dfrac{mgb - (F_{xf} + F_{xr})h_g}{a+b} \\ F_{zr} = \dfrac{mga + (F_{xf} + F_{xr})h_g}{a+b} \end{cases} \tag{3}$$

To simulate the trajectory of the vehicle, we established a ground reference coordinate system, as shown in Figure 5. Letting the coordinates of the vehicle's center of mass in the *xoy* coordinate system be *x*, *y*, and the angle between the *x′* axis of the vehicle coordinate system and the *x* axis of the ground reference coordinate system be θ. The vehicle velocity in the ground reference coordinate is projected as:

$$\begin{cases} \dot{x} = u\cos\theta - v\sin\theta \\ \dot{y} = v\cos\theta + u\sin\theta \end{cases} \tag{4}$$

The integral relationship between the course angle, sideslip angle and yaw rate can be expressed as:

$$\theta = \beta + \int \omega_r \mathrm{d}t \tag{5}$$

Take the derivative of Equation (5):

$$\dot{\theta} = \dot{\beta} + \omega_r \tag{6}$$

where $\beta = \dfrac{v}{u}$.

The differential equation of δ can be expressed as:

$$\dot{\delta} = \frac{1}{i}\delta_r \tag{7}$$

3.2. Optimal Control Model

Minimum time handling problem can be regarded as the optimal control problem. The control variables $\mathbf{Z}(t)$ is the steering wheel angle rate $\delta_r(t)$; and the control objective is to reach the terminal state in the minimum time.

Therefore, the performance index is:

$$J(Z) = \int_{t_0}^{t_e} \mathrm{d}t \tag{8}$$

The state equation can be expressed as:

$$\dot{\mathbf{X}} = f(\mathbf{X}(t), \mathbf{Z}(t)) \tag{9}$$

where $\mathbf{X}(t) = \left\{v(t)\ \omega_r(t)\ u(t)\ x(t)\ y(t)\ \theta(t)\ \delta(t)\right\}^T$

$\mathbf{Z}(t) = [\delta_r(t)]^T$.

δ and F_{xf} are constrained by the vehicle model and the road adhesion coefficient, respectively. When the vehicle is under the driving force and driven by the front wheel, the constraints on F_{xf} and F_{xr} are:

$$\begin{cases} F_{xf} \le \dfrac{\varphi mgb}{a+b+\phi h_g} \\ F_{xr} = 0 \end{cases} \tag{10}$$

When the vehicle is under a braking force, and all wheels are assumed to be in a lock-braked condition, the constraints on F_{xf} and F_{xr} are expressed as follows:

$$\begin{cases} F_{xf} \ge -\dfrac{\varphi m g_0 (b + \varphi h_g)}{a+b} \\ F_{xr} = \dfrac{a - \varphi h_g}{b + \varphi h_g} F_{xf} \end{cases} \tag{11}$$

F_{xf} is constrained by the maximum driving force. According to the driving resistance equation, the relationship between the vehicles' speed and driving force can be obtained. Assuming that the vehicle is driven by the front wheel and the driving force remains unchanged during simulation.

The constraint used to prevent rollover during the process of lane changing is (Jin *et al*., 2007; Wu *et al*., 2017):

$$\frac{u^2\delta}{(a+b)(1+Ku^2)g_0} \le \frac{B}{2h_g} \tag{12}$$

where *B* and *K* are the wheel track and the stability factor, respectively.

In order to ensure the safety during lane changing. x_f is constrained by the minimum safety distance, and y_f is constrained by the width of road centerline.

The constraint of the control variable is:

$$-\frac{\pi}{3}\,\mathrm{rad/s} \le \delta_r \le \frac{\pi}{3}\,\mathrm{rad/s}$$

The initial state and terminal state of all state variables are $\mathbf{x}(0) = [0, 0, u, 0, 0, 0, 0]$ and $\mathbf{x}(t_f) = [0, 0, u, x_f, y_f, 0, 0]$, respectively.

All the constraints are expressed as follows:

$$\boldsymbol{\psi}(\mathbf{X}(t), \mathbf{Z}(t)) = \mathbf{0} \tag{13}$$

4. SOLVING METHOD OF INVERSE DYNAMICS PROBLEM

For convenience, we summarized the inverse dynamics problem above as the optimal control problem using Mayer as the optimization objective:

$$\min\ J = \phi(\mathbf{x}(t_e),\ t_e) \tag{14a}$$

$$\text{s.t. } \dot{\mathbf{x}} = f(\mathbf{x}(t), \mathbf{z}(t), t)\quad t \in [t_0, t_e] \tag{14b}$$

$$\boldsymbol{\varphi}(x(t_0), t_0, x(t_e), t_e) = \mathbf{0} \tag{14c}$$

$$\mathbf{C}[x(t), z(t), t] \le \mathbf{0} \tag{14d}$$

where $\mathbf{x}(t) = [v(t)\ \omega_r(t)\ u(t)\ x(t)\ y(t)\ \theta(t)\ \delta(t)]^T$ $\mathbf{z}(t) = [\delta_r(t)]^T$.

Equations (14a) ~ (14d) can be obtained by the objective function, dynamic equations and constraints of the inverse dynamics problem.

The steps to solve the inverse problem of vehicle handling dynamics through GPM are as follows:

4.1. Interval Transformation

Because the collocation points of GPM are distributed in interval [−1, 1], the time interval of the optimal control problem $t \in [t_0, t_e]$ should be converted into $\tau \in [-1, 1]$ when the problem above is solved by GPM, transforming the time variable t: $\tau = (2t - (t_e + t_0))/(t_e - t_0)$, Equations (14a) ~ (14d) are converted into the following forms:

$$\min J = \psi(\mathbf{x}(\tau_e), t_e) \tag{15a}$$

$$\text{s.t. } \dot{\mathbf{x}} = \frac{t_e - t_0}{2} f(\mathbf{x}(\tau), \mathbf{z}(\tau), \tau; t_0, t_e) \tag{15b}$$

$$\boldsymbol{\varphi}(x(\tau_0), t_0, x(\tau_e), t_e) = \mathbf{0} \tag{15c}$$

$$\mathbf{C}[x(\tau), z(\tau), \tau; t_0, t_e] \le \mathbf{0} \tag{15d}$$

4.2. Global Interpolation Polynomial Approximation of State Variables and Control Variables

N LG (Legendre-Gauss) points and an initial point $\tau_0 = -1$ are selected as nodes, $N+1$ Lagrange interpolation polynomials $\mathbf{L}_i(\tau)(i = 0, \cdots, N)$ are constructed, then the state variables can be approximated using these as the basis functions:

$$\boldsymbol{x}(\tau) \approx \boldsymbol{X}(\tau) = \sum_{i=0}^{N} \boldsymbol{L}_i(\tau) \boldsymbol{X}(\tau_i) \tag{16}$$

where a Lagrange interpolation polynomial function is presented as follows:

$$\boldsymbol{L}_i(\tau) = \prod_{j=0, j\neq i}^{N} \frac{\tau - \tau_j}{\tau_i - \tau_j} \tag{17}$$

Letting the approximate states on the nodes be equal to the actual states, that is $\mathbf{x}(\tau_i) = \mathbf{X}(\tau_i)$, $(i = 0, \cdots, N)$.

The Lagrange interpolation polynomials $\mathbf{L}_i^*(\tau)$ are used as the basis functions to approximate the control variable, thus:

$$\mathbf{z}(\tau) \approx \mathbf{Z}(\tau) = \sum_{i=1}^{N} \mathbf{L}_i^*(\tau) \mathbf{Z}(\tau_i) \tag{18}$$

where $\mathbf{L}_i^*(\tau) = \prod_{j=0, j\neq i}^{N} \frac{\tau - \tau_j}{\tau_i - \tau_j}$. $\tau_i(i = 1, \cdots, N)$ are the LG points.

4.3. Convert the Dynamic Differential Equation Constraint into Algebraic Constraint

The derivative of the state variable can be obtained by taking the derivative of Equation (15), thereby converting the dynamic differential equation constraint into algebraic constraint, that is:

$$\dot{\mathbf{x}}(\tau) \approx \dot{\mathbf{X}}(\tau) = \sum_{i=0}^{N} \dot{\mathbf{L}}_i(\tau) \mathbf{X}(\tau_i) = \sum_{i=0}^{N} \mathbf{D}_{ki} \mathbf{X}(\tau_i) \tag{19}$$

The differential matrix $\mathbf{D}_{ki} \in R^{N\times(N+1)}$ is a constant value when the number of interpolation nodes is given, the expression of which is shown as follows:

$$\mathbf{D}_{ki}(\tau_k) = \dot{\mathbf{L}}(\tau_k) = \sum_{i=0}^{N} \frac{\prod_{j=0, j\neq i}^{N} (\tau_k - \tau_j)}{\prod_{j=0, j\neq i}^{N} (\tau_i - \tau_j)} \tag{20}$$

where $\tau_k(k = 1, \cdots N)$ are the points in the set κ and $\tau_i(i = 0, \cdots N)$ belong to the set $\kappa_0 = \{\tau_0, \tau_1, \cdots, \tau_N\}$. Substitute Equation (19) for Equation (14b), and convert it into the discrete state at the interpolation node $\tau_k(1 \le k \le N)$. In this way, the dynamic differential equation constraints of the optimal control problem can be converted into algebraic constraints, for $k = 1, \cdots N-1$:

$$\sum_{i=0}^{N} \mathbf{D}_{ki} \mathbf{X}(\tau_i) - \frac{\tau_e - \tau_0}{2} f(\mathbf{X}(\tau_k), \mathbf{Z}(\tau_k), \tau_k; \tau_0, \tau_e) = \mathbf{0} \tag{21}$$

4.4. Terminal State Constraint under Discrete Condition

The nodes in the GPM include N collocation points ($\tau_1, \cdots, \tau_N$), initial point $\tau_0 = -1$ and terminal point $\tau_e = 1$. The terminal state $\mathbf{X}_e$ is not defined in Equation (15), and the terminal state should also satisfy the dynamic equation constraint:

$$\mathbf{x}(\tau_e) = \mathbf{x}(\tau_0) + \int_{-1}^{1} f(\mathbf{x}(\tau), \mathbf{z}(\tau), \tau) \mathrm{d}\tau \tag{22}$$

The terminal constraint is discretized and approximated by Gaussian integration:

$$\mathbf{X}(\tau_e) = \mathbf{X}(\tau_0) + \frac{t_f - t_0}{2} \sum_{k=1}^{N} \omega_k f(\mathbf{X}(\tau_k), \mathbf{Z}(\tau_k), \tau_k; t_0, t_e) \tag{23}$$

where ω_k is the Gauss weight, and τ_k are the LG points.

The boundary value constraint (15c) and the path constraint (15d) are discretized at the interpolated points:

$$\boldsymbol{\varphi}(\mathbf{X}(\tau_0), t_0, \mathbf{X}(\tau_e), \tau_e) = \mathbf{0} \tag{24}$$

$$\mathbf{C}[\mathbf{X}(\tau_k), \mathbf{Z}(\tau_k), \tau_k; t_0, t_e] \le \mathbf{0} \tag{25}$$

The solution to the optimal control problem transformed from an inverse dynamics problem of vehicle handling is converted into solving the nonlinear programming problem through the transformation mentioned above.

5. SIMULATION ANALYSIS

5.1. Contrast Verification

In order to verify the computational accuracy of GPM, a contrast simulation is implemented.

Figures 7 (a) and (b) are the steering wheel angles obtained by GPM and DCM, respectively. In order to verify the computational accuracy of these two methods, the control variables in Figure 6 are brought into the dynamic differential equation, and state variables are obtained through explicit integration. The scatter points in Figures 7 (a) and (b) are the integral solutions. Figure 7 illustrates that these two methods are all in good agreement with the explicit integration solutions.

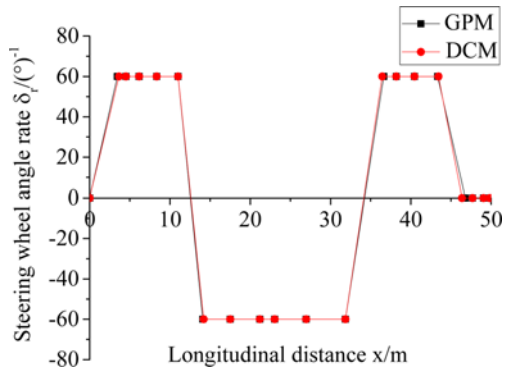

Figure 6. Control variables obtained by different methods: (a) GPM; (b) DCM.

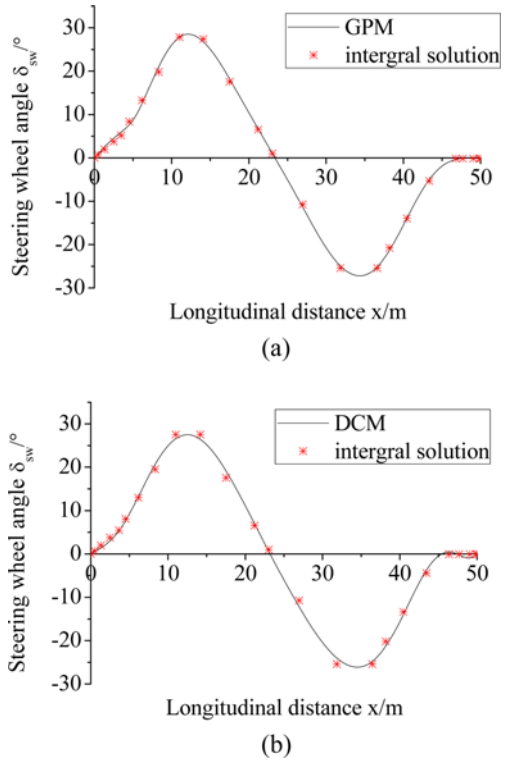

Figure 7. Simulation results of steering wheel angle: (a) Simulation results of steering wheel angle (GPM); (b) Simulation results of steering wheel angle (DCM).

All computations are performed using a 2.53 GHz/Intel Dual-core i3-380M CPU running Windows 7 with Matlab 2014a. It can be seen from Table 1 that the computational efficiency of GPM is higher than DCM, and the advantage of GPM in computational efficiency becomes more obvious as the computational accuracy increases. The computational accuracy of this paper is set to be e^{-2}. It can be seen from Figure 8 that the error between GPM and integral solutions is smaller, which indicates that the discrete and interpolation methods used by the GPM have higher accuracy.

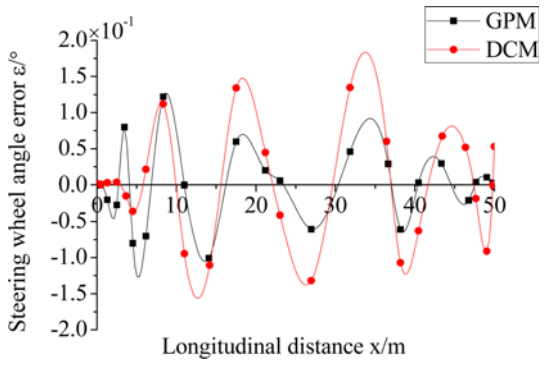

Figure 8. Comparison diagram of steering wheel angle error.

Table 1. Computational efficiency.

Computational accuracy	Method	Nodes	CPU time (s)
e^{0}	GPM	20	1.159
	DCM	20	1.226
e^{-1}	GPM	20	1.221
	DCM	20	1.299
e^{-2}	GPM	20	1.499
	DCM	20	2.099
e^{-3}	GPM	20	2.145
	DCM	20	4.976

5.2. Simulation Analysis

The moment lane changing intention occurred is taken as the initial time. The state variables of the initial time and terminal time are $\mathbf{x}(0) = [0, 0, u, 0, 0, 0, 0]$ and $\mathbf{x}(t_f) = [0, 0, u, x_f, y_f, 0, 0]$, respectively. where u and x_f are 25 m/s and 50 m, respectively. The numerical value of y_f is 3.5 m, and the sign of y_f is determined by driving intention. The model

Table 2. Model parameters.

Parameter	Value
m/kg	1500
a/m	1.2
b/m	1.3
k_1/N·rad^{-1}	− 80800
k_2/N·rad^{-1}	− 76100
I_z/kg·m^2	2500
i	20
φ	0.8
h_g/m	0.53

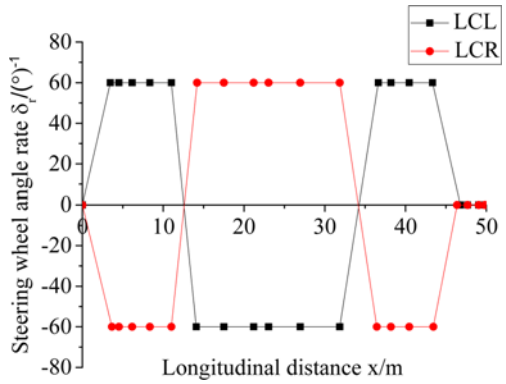

Figure 9. Simulation results of steering wheel angle rate.

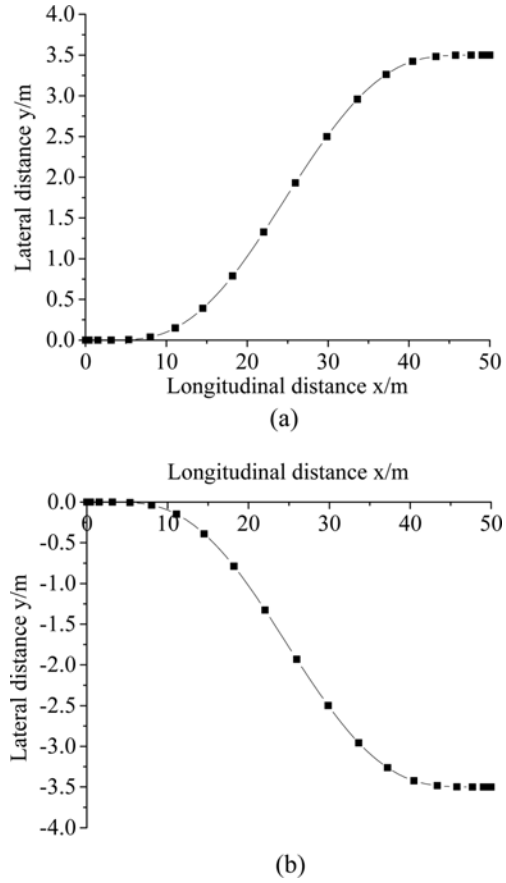

Figure 10. Simulation results of Optimal path: (a) Optimal path of LCL; (b) Optimal path of LCR.

parameters are shown in Table 2.

Figure 9 shows the simulation results of steering wheel angle rate with the minimum time as the control objective.

Figures 10 (a) and (b) are the optimal path during the process of LCL and LCR, respectively.

The steering wheel angle of minimum time lane changing is shown as Figure 11 (a), which can provide guidance for driver's lane changing behavior. Figures 11 (b) and (c) are part of vehicle state response during the process of lane changing.

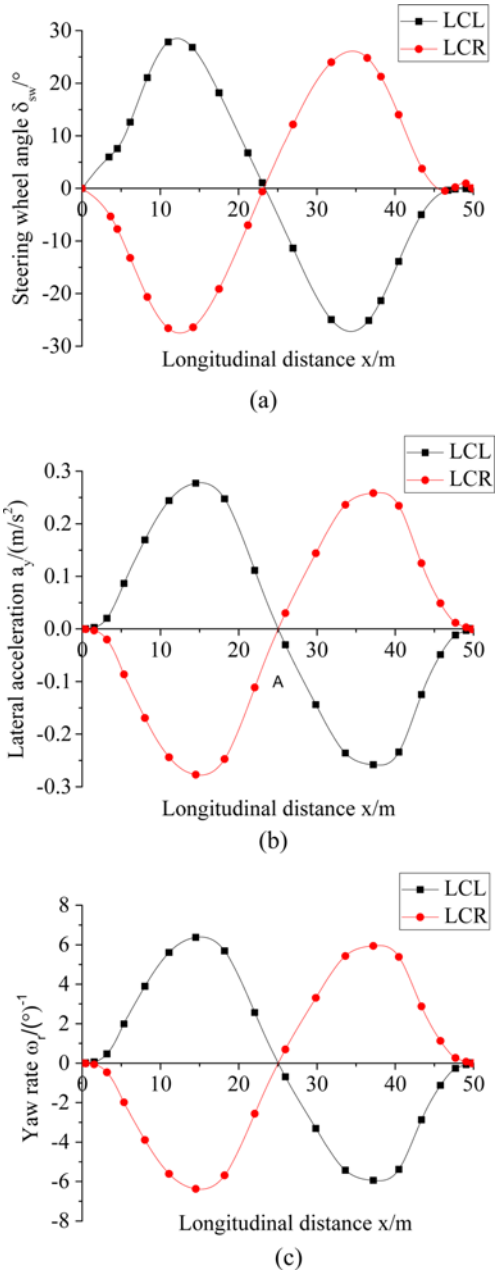

Figure 11. (a) Simulation results of steering wheel angle; (b) Simulation results of lateral acceleration; (c) Simulation results of yaw rate.

6. CONCLUSION

(1) In order to recognize driver's lane changing intention and to reduce the false alarm rate of LCAS. A hybrid lane changing intention recognition model is established based on HMM and SVM. The steering wheel angle and lateral acceleration are selected as characteristic parameters of lane changing intention

recognition model. The experimental results show that HMM-SVM hybrid model can accurately recognize the driver's lane changing intention.

(2) The inverse handling dynamics method is proposed to solve the driver's optimal handling input during lane changing. Firstly, a inverse dynamics model is established; and then the inverse dynamics problem is converted into the optimal control problem. The control objective is to complete the lane changing behavior in the minimum time. Secondly, the optimal control problem is converted into a nonlinear programming problem by GPM. Finally, the SQP method is used to solve the nonlinear programming problem. By using this method, the handling input of minimum time lane changing can be obtained without the modeling of driver.

(3) In order to verify the accuracy of GPM, the simulation results obtained by DCM were supplemented. And the accuracy of these two methods is illustrated by comparing the errors of these two methods with the explicit integral solutions. The results show that the GPM is more consistent with the integral solution, which indicates that the discrete and interpolation methods used by GPM have higher computational accuracy.

(4) A driver assistance system which can provide practical guidance for lane changing handling input is constructed. It is helpful to avoid traffic accidents caused by driver's improper handling. This study can not only improve the safety during lane changing, but also provide some references for unmanned vehicles.

ACKNOWLEDGEMENT–This work is supported by the National Natural Science Foundation of China (grant numbers 11672127, 51605215), the Major Exploration Project of the General Armaments Department of China (grant numbers NHA13002) the Fundamental Research Funds for the Central Universities (grant numbers NP2016412, NP2018403, NT2018002). and the Postgraduate Research & Practice Innovation Program of Jiangsu Province (Grant No. KYCX17_0240).

REFERENCES

Andreasson, J. and Bunte, T. (2006). Global chassis control based on inverse vehicle dynamics models. *Vehicle System Dynamics: Int. J. Vehicle Mechanics and Mobility* **44**, **Supplement 1**, 321–328.

Bernard, J. and Pickelmann, M. (1986). An inverse linear model of a vehicle. *Vehicle System Dynamics: Int. J. Vehicle Mechanics and Mobility* **15**, **4**, 179–186.

Berndt, H. and Dietmayer, K. (2009). Driver intention inference with vehicle onboard sensors. *Proc. IEEE Int. Conf. Vehicular Electronics and Safety (ICVES)*, Pune, India.

Boyer, F. and Ali, S. (2011). Recursive inverse dynamics of mobile multibody systems with joints and wheels. *IEEE Trans. Robotics* **27**, **2**, 215–228.

Casanova, D., Sharp, R. S. and Symonds, P. (2000). Minimum time maneuvering: the significance of yaw inertia. *Vehicle System Dynamics: Int. J. Vehicle Mechanics and Mobility* **34**, **2**, 77–115.

Chovan, J. D., Tijerina, L., Alexander, G. and Hendricks, D. L. (1994). Examination of Lane Change Crashes and Potential IVHS Countermeasures. NHTSA Technical Report. DOT -VNTSC-NHTSA-93-2.

Cole, D. J. (2012). A path-following driver-vehicle model with neuromuscular dynamics, including measured and simulated responses to a step in steering angle overlay. *Vehicle System Dynamics: Int. J. Vehicle Mechanics and Mobility* **50**, **4**, 573–596.

Dang, R. N., Zhang, F., Wang, J. Q., Yi, S. C. and Li, K. Q. (2013). Analysis of Chinese driver's lane change characteristic based on real vehicle tests in highway. *Proc. 16th Int. IEEE Conf. Intelligent Transportation Systems*, Hague, Netherlands.

Doga, U., Edelbrunner, J. and Iossifidis, I. (2011). Autonomous driving: A comparison of machine learning techniques by means of the prediction of lane change behavior. *Proc. IEEE Int. Conf. Robotics and Biomimetics*, Karon Beach, Phuket, Thailand.

Eidehall, A., Pohl, J. and Gustafsson, F. (2005). A new approach to lane guidance systems. *Proc. IEEE Intelligent Transportation Systems*, Vienna, Austria.

Fujioka, T. and Kimura, T. (1992). Numerical simulation of minimum-time cornering behavior. *JSAE Review* **13**, **1**, 44–51.

Gadepally, V., Krishnamurthy, A. and Ozguner, U. (2014). A framework for estimating driver decisions near intersections. *IEEE Trans. Intelligent Transportation Systems* **15**, **2**, 637–646.

Garg, D., Hager, W. W. and Rao, A. V. (2011). Pseudospectral methods for solving infinite-horizon optimal control problems. *Automatica* **47**, **4**, 829–837.

Gipps, P. G. (1986). A model for the structure of lane-changing decisions. *Transportation Research Part B: Methodological* **20**, **5**, 403–414.

Guo, J. H., Hu, P. and Wang, R. B. (2016). Nonlinear coordinated steering and braking control of vision-based autonomous vehicles in emergency obstacle avoidance. *IEEE Trans. Intelligent Transportation Systems* **17**, **11**, 3230–3240.

Guo, J. H., Hu, P., Li, L. H. and Wang, R. B. (2012). Design of automatic steering controller for trajectory tracking of unmanned vehicles using genetic algorithms. *IEEE Trans. Vehicular Technology* **61**, **7**, 2913–2924.

Guo, J. H., Luo, Y. G. and Li, K. Q. (2018a). Adaptive coordinated collision avoidance control of autonomous ground vehicles. *Proc. Institution of Mechanical Engineers, Part I: J. Systems and Control Engineering*, DOI: https://doi.org/10.1177/0959651818774991.

Guo, J. H., Luo, Y. G. and Li, K. Q. (2018b). Adaptive nonlinear trajectory tracking control for lane change of

autonomous four wheel independently drive electric vehicles. *IET Intelligent Transport Systems* **12**, **7**, 712–720.

Guo, J. H., Luo, Y. G., Li, K. Q. and Dai, Y. F. (2018c). Coordinated path-following and direct yaw-moment control of autonomous electric vehicles with sideslip angle estimation. *Mechanical Systems and Signal Processing*, **105**, 183–199.

Guo, K. H. (1984). Drivers-vehicle close-loop simulation of handling by "preselect optimal curvature method". *Automotive Engineering*, **3**, 1–17.

Hendrikx, J. P. M., Meijlink, T. J. J. and Kriens, R. F. C. (1996). Application of optimal control theory to inverse simulation of car handling. *Vehicle System Dynamics: Int. J. Vehicle Mechanics and Mobility* **26**, **6**, 449–461.

Hidas, P. (2002). Modeling lane changing and merging in microscopic traffic simulation. *Transportation Research Part C: Emerging Technologies* **10**, **5-6**, 351–371.

Hou, Y., Edara, P. and Sun, C. (2014). Modeling mandatory lane changing using Bayes classifier and decision trees. *IEEE Trans. Intelligent Transportation Systems* **15**, **2**, 647–655.

Jin, Z. L., Weng, J. S. and Hu, H. Y. (2007). Rollover stability of a vehicle during critical driving maneuvers. *Proc. Institution of Mechanical Engineers, Part D: J. Automobile Engineering* **221**, **9**, 1041–1049.

Jula, H., Kosmatopoulos, E. B. and Ioannou, P. (2000). Collision avoidance analysis for lane changing and merging. *IEEE Trans. Vehicular Technology* **49**, **6**, 2295–2308.

Lee, S. E., Olsen, E. C. B. and Wierwille, W. W. (2004). A Comprehensive Examination of Naturalistic Lane-changes. NHTSA Technical Report. DOT-HS-809-702.

Li, K. Q., Wang, X., Xu, Y. C. and Wang, J. Q. (2016). Lane changing intention recognition based on speech recognition models. *Transportation Research Part C: Emerging Technologies*, **69**, 497–514.

Liu, Y. J. and Jiang, J. S. (2016). Optimum path tracking control for inverse problem of vehicle handling dynamics. *J. Mechanical Science and Technology* **30**, **8**, 3433–3440.

Mccall, J. C., Trivedi, M. M., Wipf, D. and Rao, B. (2007). Lane change intent analysis using robust operators and sparse bayesian learning. *IEEE Trans. Intelligent Transportation Systems* **8**, **3**, 431–440.

Na, X. X. and Cole, D. J. (2015). Game-theoretic modeling of the steering interaction between a human driver and a vehicle collision avoidance controller. *IEEE Trans. Human-Machine Systems* **45**, **1**, 25–38.

NHTSA (2017). Traffic Safety Facts 2015. NHTSA Technical Report. DOT-HS-812-384.

Ruder, M., Enkelmann, W. and Garnitz, R. (2002). Highway Lane Change Assistant. *Proc. IEEE Intelligent Vehicle Symp*., Versailles, France.

Stein, G. P., Mano, O. and Shashua, A. (2000). A robust method for computing vehicle ego-motion. *Proc. IEEE Intelligent Vehicles Symp*., Dearborn, Michigan, USA.

Van Dijck, T. and Van Der Heijden, G. A. J. (2005). Vision Sense-an advanced lateral collision avoidance warning system. *Proc. IEEE Intelligent Vehicles Symp*., Las Vegas, Nevada, USA.

Wang, J. X., Zhang, G. G., Wang, R. R., Schnelle, S. C. and Wang, J. M. (2017). A gain-scheduling driver assistance trajectory-following algorithm considering different driver steering characteristics. *IEEE Trans. Intelligent Transportation Systems* **18**, **5**, 1097–1108.

Wang, W., Bei, S. Y., Yang, H. and Zhang, L. C. (2015). Minimum time approach to emergency collision avoidance by vehicle handling inverse dynamics. *Mathematical Problems in Engineering*, **2015**, Article ID 276460, 1–9.

Wang, W., Zhao, Y. Q., Bei, S. Y., Liu, W. T. and Xu, J. X. (2014). Controlling and optimization of vehicle while encountering an emergency collision avoidance. *J. Vibroengineering* **16**, **2**, 623–632.

Wu, J., Cheng, S., Liu, B. H. and Liu, C. Z. (2017). A human-machine-cooperative-driving controller based on AFS and DYC for vehicle dynamic stability. *Energie* **10**, **11**, 1–18.

Xia, X., Xiong, L., Hou, Y. Y., Teng, G. W. and Yu, Z. P. (2017). Vehicle stability control based on driver's emergency alignment intention recognition. *Int. J. Automotive Technology* **18**, **6**, 993–1006.

Xiong, L., Teng, G. W., Yu, Z. P., Zhang, W. X. and Feng, Y. (2016). Novel stability control strategy for distributed drive electric vehicle based on driver operation intention. *Int. J. Automotive Technology* **17**, **4**, 651–663.

Yang, Q. and Koutsopoulos, H. N. (1996). A microscopic traffic simulator for evaluation of dynamic traffic management systems. *Transportation Research Part C: Emerging Technologies* **4**, **3**, 113–129.

Yang, X. K. and Zhou, H. G. (2004). CORSIM-based simulation approach to evaluation of direct left turn versus right turn plus U-turn from driveways. *J. Transportation Engineering* **130**, **1**, 68–75.

Zhang, Y. L., Owen, L. E. and Clark, J. (1998). Multiregime approach for microscopic traffic simulation. *Transportation Research Record: J. Transportation Research Board* **1644**, **1**, 103–115.

Zong, C. F., Wang, C., Yang, D. and Yang, H. (2009). Driving intention identification and maneuvering behavior prediction of drivers on cornering. *Proc. IEEE Int. Conf. Mechatronics and Automation*, Changchun, China.